

---

# Measurement of Dopamine Release with Continuous Infusion of [<sup>11</sup>C]Raclopride: Optimization and Signal-to-Noise Considerations

Hiroshi Watabe, Christopher J. Endres, Alan Breier, Bernard Schmall, William C. Eckelman, and Richard E. Carson

*PET Department, Clinical Center, and Experimental Therapeutics Branch, National Institute of Mental Health, National Institutes of Health, Bethesda, Maryland*

---

PET studies with [<sup>11</sup>C]raclopride provide an indirect measure of changes in synaptic dopamine. Previously, we used the bolus-plus-infusion (B/I) method to assess dopamine response from the percentage change in binding potential ( $\Delta$ BP) before and after administration of amphetamine. The goal of this work is to optimize the measurement of changes in neurotransmitter with the B/I method by choosing the optimal timing for pre- and poststimulus scanning. **Methods:** Two sources of variability in  $\Delta$ BP were considered: within-subject and between-subject noise. A noise model based on a phantom study and human data was used to evaluate the within-subject noise. For between-subject noise, simulated time-activity curves were generated from measured [<sup>11</sup>C]raclopride input functions. Optimal timing to measure  $\Delta$ BP was determined and applied to human data. **Results:** According to the simulation study, the optimal scan times for pre- and poststimulus scans were 39–50 and 58–100 min, respectively. The optimal timing resulted in a 28% noise reduction compared with the original timing. By applying the optimal timing to human studies, the statistical significance of the difference in  $\Delta$ BP between patients with schizophrenia and healthy volunteers increased from  $P = 0.038$  to 0.012. **Conclusion:** Careful assessment of the sources of noise in receptor imaging studies can increase the sensitivity of the B/I method for the detection of biologic signals.

**Key Words:** [<sup>11</sup>C]raclopride; bolus/infusion; amphetamine; noise; optimization

**J Nucl Med 2000; 41:522–530**

---

**C**hanges in the dopamine system are an important component in several diseases, such as Parkinson's disease and schizophrenia. Using PET or SPECT with receptor-specific radioligands, dynamic changes in neurotransmitter concentrations can be detected in vivo in the human brain. One experimental paradigm that has been studied extensively is the amphetamine-induced increase in synaptic dopamine by its release from cytosolic stores (1). Amphetamine-induced dopamine release has been measured using

PET and SPECT with [<sup>11</sup>C]raclopride and [<sup>123</sup>I]iodobenzamide (IBZM) (2–7) with 2 approaches. The first is to use 2 studies with bolus injections—i.e., a control study usually followed by a stimulus study. Receptor-related parameters such as the distribution volume are measured in each study, and the change between the 2 studies is determined (8). Another approach is to use a bolus-plus-infusion (B/I) study (9) that requires only a single radiopharmaceutical administration. Using the B/I method, Laruelle et al. (5) and Breier et al. (6) showed that patients with schizophrenia produced a larger elevation in synaptic dopamine than did control subjects after amphetamine.

The B/I method has the advantage of simplicity over the dual-bolus injection approach. With this method, tracer administration commences and an equilibrium level of tracer is reached. The baseline binding potential (BP) is determined from concentration ratios of regions with and without specific binding. Then, a stimulus is administered, which causes a change in the tracer level that is due to competition with an altered concentration of endogenous neurotransmitter. At an appropriate time poststimulus, the BP is measured and the stimulus-induced percentage change in BP,  $\Delta$ BP, is calculated. The choice of timing of the pre- and poststimulus measurements of BP can greatly affect the signal and noise characteristics of this measurement.

The goal of this work is to maximize the signal-to-noise ratio (SNR) of the measurement of  $\Delta$ BP with a B/I study and [<sup>11</sup>C]raclopride to improve the sensitivity of this method for detecting group differences in dopamine release while maintaining the simple ratio methods. Two sources of noise are considered. The first is within-subject variability associated with statistical noise in the PET measurements. To describe this noise, a phantom study was performed and a noise model was developed (Appendix A). The second source of variability is between-subject error. One component of this error is population variation in neurotransmitter release across subjects, an effect that cannot be controlled. In addition, the B/I method will contribute subject-to-subject variation associated with individual biases in the measurement of pre- and poststimulus BP. Ideally, a B/I study produces constant levels of radioactivity throughout the

---

Received Dec. 14, 1998; revision accepted Jul. 14, 1999.

For correspondence or reprints contact: Richard E. Carson, PhD, PET Department, National Institutes of Health, Bldg. 10, Rm. 1C-401, 10 Center Dr., MSC 1180, Bethesda, MD 20892-1180.

brain and the prestimulus BP will be accurately measured. However, because of individual differences in tracer clearance and kinetic parameters, ideal equilibrium will not be attained in all subjects when a standard B/I administration is used. To assess this error, we used measured [<sup>11</sup>C]raclopride plasma input functions and simulated brain time-activity curves using an extended receptor kinetic model (10) that includes the effect of transient changes in endogenous neurotransmitters. Given these models for variability in ΔBP, optimal timing for the pre- and poststimulus measurements was determined and then applied to previously collected data, comparing amphetamine-induced dopamine release in patients with schizophrenia with that in healthy volunteers.

## MATERIALS AND METHODS

### PET Studies

Data were taken from PET studies in humans as described previously (6). There were 12 healthy volunteers (age, 32.4 ± 3.0 y) and 11 patients with schizophrenia (age, 29.2 ± 2.6 y). Briefly, subjects were administered [<sup>11</sup>C]raclopride (74–296 MBq [2–8 mCi]) as a bolus followed by constant infusion (B/I). The bolus volume was 57% of the total volume in the injection syringe. Because of radioactive decay, the bolus accounted for 83% of the radiation dose. Twenty-seven scan frames were acquired in 3-dimensional mode over 100 min. At 50 min, amphetamine (0.2 mg/kg) was infused intravenously over 60 s.

Under equilibrium conditions, BP can be obtained directly from the radioactivity concentration of the receptor-rich or target region (C[nCi/mL]) and a receptor-poor or background region (C'[nCi/mL]) as the ratio BP = (C - C')/C' (10,11). BP equals the equilibrium ratio of bound ligand (C<sub>b</sub>[nCi/mL]) to free plus nonspecifically bound tracer (C<sub>f</sub>[nCi/mL]) under the assumption that nonspecific binding is uniform throughout the brain. Therefore, the percentage change in BP (ΔBP) caused by a stimulus (e.g., amphetamine) is defined as:

$$\Delta BP = \frac{\left(\frac{C_{pre} - C'_{pre}}{C'_{pre}}\right) - \left(\frac{C_{post} - C'_{post}}{C'_{post}}\right)}{\frac{C_{pre} - C'_{pre}}{C'_{pre}}} \times 100 (\%), \quad \text{Eq. 1}$$

where pre and post refer to time periods before and after the stimulus, respectively. The quantity ΔBP has been shown to be proportional to the integral of the free dopamine pulse—i.e., the time course of dopamine released by amphetamine normalized by the K<sub>d</sub> of dopamine—based on simulation studies derived from simultaneous [<sup>11</sup>C]raclopride PET and microdialysis experiments in monkeys (10,12).

C and C' were calculated from volume-of-interest (VOI) values averaged over a few scan frames in the target region (left and right basal ganglia) and background region (cerebellum), respectively. In the original human studies, ΔBP was calculated by averaging C and C' over 5 frames over 30–50 min (pre) and 75–100 min (post) (6).

Additionally, a phantom study was performed to develop a noise model for ΔBP. A cylindrical phantom with two 3-cm-diameter spheres, simulating the basal ganglia, was used. Full details of the phantom study and the resulting noise model are presented in Appendix A.

To evaluate the accuracy of the noise model, comparisons between the predicted error and measured error of ΔBP were

carried out. Data from 16 human studies were used. VOIs that trace the target region (basal ganglia) and background region (cerebellum) were placed on summed images (0–100 min) of each dynamic study. Time-activity curves for target and background regions were computed. For each subject, the mean values for C and C' and their ratio (R) for time periods (5 scan frames each) before amphetamine (30–50 min) and after amphetamine (75–100 min) were calculated. Assuming constant radioactivity values during these periods, measured target and background region noise was estimated from the 5 time points, and the measured error of ΔBP was determined from these sample values and a propagation of errors analysis applied to Equation 1 (Appendix A). These measured errors were compared with the noise model prediction of the error of ΔBP. For each subject, the measured noise equivalent count rate (NECR) (13,14) values during 30–50 min and 75–100 min and the number of pixels in each VOI were used.

### Extended Receptor Model

To analyze a neurotransmitter competition study, the conventional tracer kinetic model for receptor-binding radiopharmaceuticals (15) was previously extended to include time-varying changes in neurotransmitter concentration (10). As in the conventional model, this model has 2 compartments: C<sub>f</sub> and C<sub>b</sub>. The model differential equations are:

$$\frac{dC_f}{dt} = K_1 C_p - (k_2 + k_3(t))C_f + k_4 C_b, \quad \text{Eq. 2}$$

$$\frac{dC_b}{dt} = k_3(t)C_f - k_4 C_b, \quad \text{Eq. 3}$$

where K<sub>1</sub> is the plasma-to-tissue influx rate constant (mL/min/mL), k<sub>2</sub> is the tissue-to-plasma rate constant (min<sup>-1</sup>), and k<sub>4</sub> is the dissociation rate constant (min<sup>-1</sup>). Under conditions of constant receptor occupancy, k<sub>3</sub> is the binding rate constant (min<sup>-1</sup>); however, in the presence of a time-varying dopamine pulse, k<sub>3</sub> is time dependent—i.e., k<sub>3</sub>(t).

Assuming the free and bound dopamine are in equilibrium, k<sub>3</sub>(t) can be expressed as (10):

$$k_3(t) = \frac{k_3^{pre}}{1 + \frac{D_f(t)}{K_d^{DA}}}, \quad \text{Eq. 4}$$

where k<sub>3</sub><sup>pre</sup> is the k<sub>3</sub> value before the stimulus is administered, D<sub>f</sub>(t) is the free dopamine concentration (nmol/L) at time t, and K<sub>d</sub><sup>DA</sup> is the equilibrium dissociation constant for dopamine (nmol/L). Equation 4 assumes that dopamine binds to the D<sub>2</sub> receptors with a single affinity. Based on microdialysis data (10), D<sub>f</sub>(t)/K<sub>d</sub><sup>DA</sup> in Equation 4 can be expressed as follows:

$$\begin{aligned} \frac{D_f(t)}{K_d^{DA}} &= 0 & t < t_{stim} \\ &= h \exp(-r(t - t_{stim})) & t > t_{stim}, \end{aligned} \quad \text{Eq. 5}$$

where t<sub>stim</sub> is the time (min) when the stimulus (amphetamine) is applied. Baseline levels of dopamine are ignored in this formulation because that factor can be incorporated into k<sub>3</sub><sup>pre</sup> and K<sub>d</sub><sup>DA</sup> (12). A 4th-order Runge-Kutta algorithm (16) was used to solve the differential equations.

## Simulation Study

Ideally, to achieve an equilibrium state in all tissues by the B/I method, a bolus study would be required for each subject to determine the ideal infusion schedule. However, for clinical practicality, a fixed infusion protocol was used, and, thus, ideal equilibrium will not be produced for all subjects. To model this variability in simulations of the B/I method, several different input functions must be used. We used plasma radioactivity data from 11 subjects acquired during [<sup>11</sup>C]raclopride PET scanning with the B/I method. Because of insufficient statistics in individual measurements of plasma metabolites for [<sup>11</sup>C]raclopride, literature values for the rate of plasma metabolism were applied to these data (17). Because those data were collected from bolus experiments, the data were transformed to account for B/I tracer delivery (Appendix B).

From the 11 metabolite-corrected plasma input curves, noise-free time-activity curves of 100-min duration for the target and background regions were generated based on the extended receptor model. The kinetic parameters were  $K_1 = 0.11$  mL/min/mL,  $k_2 = 0.278$ /min,  $k_3^{\text{pre}} = 0.300$ /min, and  $k_4 = 0.108$ /min (15), and the dopamine pulse parameters were  $h = 1$  and  $r = 0.06$ /min (10) for the target region, where  $h$  and  $r$  indicate normalized height and clearance rate (/min) for the dopamine pulse. For the background region with no specific binding, the kinetic parameters were  $K_1' = 0.11$  mL/min/mL and  $k_2' = 0.278$ /min. Noise was added to the target and background time-activity curves using the noise model (Appendix A) and the average human NECR data. For the noise calculation, the sizes of the VOIs were determined from the average sizes from 16 subjects as 1044 and 3562 pixels for the target (left and right basal ganglia) and background (cerebellum) regions, respectively.

## Optimal Timing for $\Delta$ BP

In our original study (6),  $\Delta$ BP in Equation 1 was calculated using data from 30 to 50 min and 75 to 100 min for pre- and poststimulus values, respectively. These times were chosen on the basis of visual inspection of the time-activity curves. To improve the SNR of  $\Delta$ BP, we determined optimal timing for the tissue concentration measurements. The total noise in  $\Delta$ BP,  $\sigma_{\text{total}}(\Delta\text{BP})$ , is defined as  $\sqrt{\sigma_{\text{within}}^2 + \sigma_{\text{between}}^2}$ , where  $\sigma_{\text{within}}$  and  $\sigma_{\text{between}}$  are within-subject and between-subject errors, respectively. Within-subject error refers to the statistical noise in  $\Delta$ BP (Appendix A). Between-subject error is obtained from the variance of  $\Delta$ BP among subjects in the simulation study. Four parameters,  $t_{\text{pre}}$ ,  $\Delta_{\text{pre}}$ ,  $t_{\text{post}}$ , and  $\Delta_{\text{post}}$ , reflecting the start times and durations (min) of the pre- and poststimulus time periods, were varied to minimize the coefficient of variation  $\sigma_{\text{total}}/\Delta\text{BP}$  by means of the downhill simplex method (16). This method is a robust minimization method using a simplex consisting of  $n + 1$  points in an  $n$ -dimensional parameter space. The simplex method is useful for this problem because it does not require calculation of function derivatives. For application to the previous studies, constraints of  $t_{\text{pre}} + \Delta_{\text{pre}} \leq 50$  min and  $t_{\text{post}} + \Delta_{\text{post}} \leq 100$  min were applied.

## Application of Optimal Timing to Human Studies

We applied the optimal timing obtained from the simulation study to the data of Breier et al. (6), which had shown a statistically significant difference in  $\Delta$ BP between healthy volunteers and patients with schizophrenia. The time-activity curves for basal ganglia and cerebellum produced in the previous analysis were used to calculate  $\Delta$ BP with the original and optimal timings.

## RESULTS

The following equation was derived for the SD of  $\Delta$ BP (Appendix A):

$$\text{SD}(\Delta\text{BP}) = 192,000 \frac{R_{\text{post}} - 1}{R_{\text{pre}} - 1} \times \sqrt{\frac{\left(\frac{1}{R_{\text{pre}}^{1.61}n} + \frac{4.34}{n^{1.35}}\right)}{\text{NEC}_{\text{pre}}(1 - R_{\text{pre}}^{-1})^2} + \frac{\left(\frac{1}{R_{\text{post}}^{1.61}n} + \frac{4.34}{n^{1.35}}\right)}{\text{NEC}_{\text{post}}(1 - R_{\text{post}}^{-1})^2}}, \quad \text{Eq. 6}$$

where  $\text{NEC}_{\text{pre}}$  and  $\text{NEC}_{\text{post}}$  are the summed noise equivalent count (NEC) values for the pre- and poststimulus time periods, respectively;  $R_{\text{pre}}$  and  $R_{\text{post}}$  are the target-to-background concentration ratios before and after stimulus, respectively; and  $n$  and  $n'$  are the number of pixels in the target and background VOIs, respectively.

Figure 1 shows the comparison between measured and predicted  $\text{SD}(\Delta\text{BP})$  values for 16 human subjects. There was very good agreement between the observed and predicted values ( $\text{SD}_{\text{pred}} = 1.03\text{SD}_{\text{obs}} - 0.26$ ;  $r = 0.917$ ). The wide range of  $\text{SD}(\Delta\text{BP})$  values is produced by interindividual differences in injected radioactivity and body weight.

Analysis of Equation 6 indicates that the noise contribution of the background region to  $\Delta$ BP is substantial. For example, substituting mean values of human studies ( $R_{\text{pre}} = 3.68$ ,  $R_{\text{post}} = 3.24$ ,  $\text{NEC}_{\text{pre}} = 1.14 \times 10^7$ ,  $\text{NEC}_{\text{post}} = 3.53 \times 10^6$ ,  $n = 1044$ , and  $n' = 3562$ ) into Equation 6,  $\Delta$ BP is 16.4% and  $\text{SD}(\Delta\text{BP})$  is 2.03 or 12.4% of  $\Delta$ BP. If

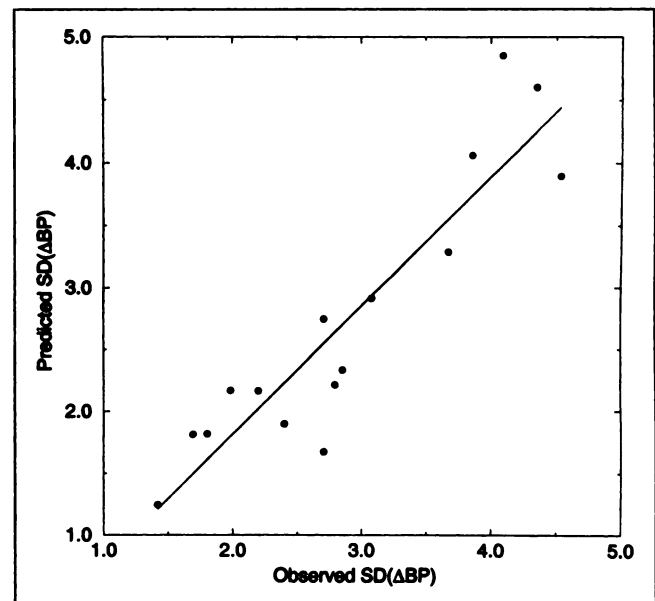


**FIGURE 1.** Comparison between observed and predicted  $\text{SD}(\Delta\text{BP})$  from data of 16 human subjects.  $\Delta$ BP was calculated using data from basal ganglia and cerebellum during 30–50 min and 75–100 min. Observed  $\text{SD}$  values were determined from  $\Delta$ BP values taken from individual scans during each period. Predicted  $\text{SD}(\Delta\text{BP})$  was taken from Equation 6. Solid line is regression line,  $\text{SD}_{\text{pred}} = 1.03\text{SD}_{\text{obs}} - 0.26$ ;  $r = 0.917$ .

the noise in the background region was eliminated (by setting the pixel number  $n'$  to infinity), the %SD of  $\Delta BP$  drops to 10.0 from 12.4%, a reduction of 19%. If  $n'$  were reduced by 40%, the noise contribution of the background region would in fact be equal to that of the target region. Thus, the background region should be as large as is reasonably possible to minimize  $SD(\Delta BP)$ .

#### Optimal Timing for $\Delta BP$

Figure 2 shows examples of noise-free simulated time-activity curves of target and background regions. In these simulations, only measured total plasma radioactivity curves were varied. Fixed kinetic parameters and plasma metabolite rates were used to simulate the time-activity curves. Nevertheless, we observed different shapes of the resulting curves,

and constant radioactivity levels were not achieved in all curves. The slopes of the target region curves from 30 to 50 min were  $-0.168 \pm 0.152 \%/min$  for the simulation studies, which was very similar to values of  $-0.154 \pm 0.168 \%/min$  for the human studies. This similarity suggests that the simulation of interindividual variability is adequate despite the use of fixed kinetic parameters and an average metabolite correction. The negative slope suggests that the infusion protocol could be improved (see Discussion section).

Table 1 shows the results of optimal timing for  $\Delta BP$  from the simulation study—i.e., mean  $\Delta BP$  values and total noise  $\sigma_{total}$  obtained by the original and optimal timing. It also shows the normalized within- and between-subject noise of  $\Delta BP$ . The optimization shortened the prestimulus scan times

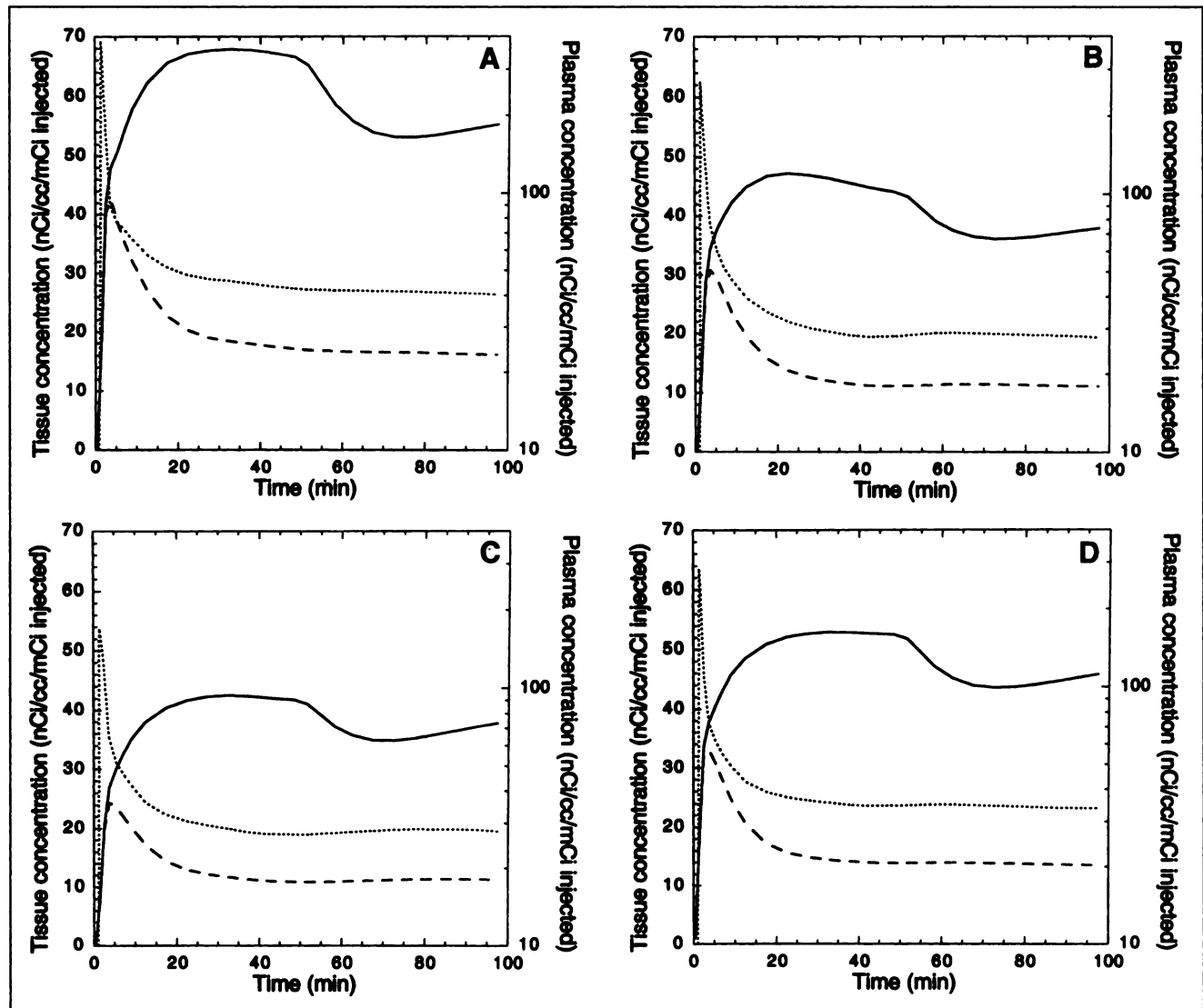


**FIGURE 2.** Examples of simulated time-activity curves from measured human plasma input functions. All data are expressed in normalized units of nCi/mL/mCi injected. Plasma data (dotted line) were corrected for metabolites by mean population values (Appendix B). Time-activity curves for target region (solid line) were generated based on the extended kinetic model with parameters of  $K_1 = 0.11$  mL/min/mL,  $k_2 = 0.278$ /min,  $k_3^{re} = 0.300$ /min,  $k_4 = 0.108$ /min,  $h = 1$ , and  $r = 0.06$ /min. Time-activity curves for background region (dashed line) were generated using a 1-tissue compartment model with parameters of  $K_1' = 0.11$  mL/min/mL and  $k_2' = 0.278$ /min.

**TABLE 1**  
Optimal Timing for  $\Delta$ BP

Method	Timing (min)		Mean $\Delta$ BP	%SD			
	Pre	Post		$\sigma_{total}$	$\sigma_{within}$	$\sigma_{between}$	$\sigma_{total}$
Original	30–50	75–100	19.2	3.5	9.4	15.8	18.4
Optimal	39–50	58–100	21.0	2.8	7.1	11.2	13.3

from 30–50 min to 39–50 min. This provides additional time for equilibrium to be reached and has the effect of reducing between-subject error from 15.8% to 11.2% by reducing the effects of lack of equilibrium. For the poststimulus period, the optimal time period was extended from 75–100 min to 58–100 min. By taking data longer, statistical noise is suppressed—i.e., within-subject error was reduced from 9.4% to 7.1%. By this optimization process, a 28% improvement in the SNR for  $\Delta$ BP was obtained compared with original timing. Such an improvement can have an important impact on the design of a study to compare groups—i.e., an increase in signal to noise can be thought of as an increase in the number of subjects. As shown in Table 1, the mean  $\Delta$ BP value was increased by the optimization from 19.2 to 21.0. The main reason for this increase was that  $R_{pre}$  was increased primarily because of a 2.4% reduction in  $C'_{pre}$ , because the optimization excluded data (30–39 min) where the time-activity curves had not yet reached equilibrium.

#### Application of Optimal Timing to Human Studies

Table 2 and Figure 3 show the results from application of the optimal timing to the comparison of [ $^{11}$ C]raclopride  $\Delta$ BP between healthy control subjects and patients with schizophrenia (6). Application of the new timing had a number of effects on the data. First, the mean value of  $\Delta$ BP was reduced in both groups. This differed from the results of the simulation, probably because of differences in the postamphetamine data (see Discussion section). Second, as expected, the SD of  $\Delta$ BP values in the control group was reduced from 6.1 to 5.1. The reduction in  $\Delta$ BP was less noticeable in the patient group because the original intersubject variance was much larger than that of the healthy volunteers. Finally, statistical tests were performed to compare the healthy volunteers and patients with schizophrenia (unpaired  $t$  test). The  $t$  value using the original timing was 2.21 and the  $t$  value

**TABLE 2**  
 $\Delta$ BP for Healthy Volunteers ( $n = 12$ ) and Patients with Schizophrenia ( $n = 11$ ) Obtained by Original Timing and Optimal Timing

Group	Original	Optimal
Healthy volunteers	15.4 $\pm$ 6.1	11.8 $\pm$ 5.1
Schizophrenic patients	22.9 $\pm$ 10.0	20.6 $\pm$ 9.7
$P$	0.038	0.012

Data are presented as mean  $\pm$  SD.

for the optimized data was 2.77. Thus, the optimal timing increased the  $t$  value by 25% so that the statistical significance of the difference between healthy volunteers and patients with schizophrenia was increased—i.e., the probability value dropped from 0.038 to 0.012. To have reached the same probability value with original timing, the number of subjects would have to be increased from 12 to 17—i.e., a 42% increase in the sample size.

## DISCUSSION

The measurement of dynamic change in neurotransmitter level in the living human brain with PET or SPECT can be a powerful tool in neuroscience. To detect the small signals produced by neurotransmitter release, experiments must be carefully designed, and the method of data collection and analysis can significantly affect the results. To increase the sensitivity to neurotransmitter release with PET, we must reduce noise in the data wherever possible. This is particularly important if analysis of very small brain volumes is attempted. For [ $^{11}$ C]raclopride, with its short half-life and faster kinetics than [ $^{123}$ I]IBZM, small changes in the B/I method may substantially affect its signal-to-noise characteristics. We therefore investigated several controllable noise sources and evaluated an optimized design for B/I experiments.

#### Optimization of Method

We used the downhill simplex method to estimate optimal timing to measure  $\Delta$ BP. In addition to estimating the best pre- and poststimulus scan intervals, we could also optimize the time that the stimulus is administered. If this time value is longer than 50 min, there would be more time to achieve equilibrium before the stimulus. However, statistical noise would be increased for the poststimulus data. An optimization, including the estimation of the best administration time of the stimulus (with total experiment time fixed at 100 min), resulted in  $t_{stim} = 59$  min with pre- and poststimulus scanning starting at 36 and 68 min, respectively. Because the time of the administration of the stimulus is longer than 50 min, the prestimulus interval is longer and suppresses within-subject noise because of lack of equilibrium. Although within-subject noise increases because of the shortened poststimulus interval, the net effect is improved signal to noise.

In the simulation, the optimal timing caused a slight increase in  $\Delta$ BP (Table 1). However in the human data,  $\Delta$ BP values were decreased by applying the optimal timing (Table 2). This effect was produced primarily by changes in the  $R_{post}$  values. Timing optimization increased  $R_{pre}$  values by 1.5%  $\pm$  0.7% and 0.6%  $\pm$  1.9% for the simulation and human studies, respectively.  $R_{post}$  values were changed by  $-0.1\% \pm 0.7\%$  and  $+3.0\% \pm 2.0\%$  for the simulation and human data, respectively. The increase in  $R_{post}$  in the human data produced the decrease in  $\Delta$ BP. There are a number of possible reasons for this discrepancy. In the simulation, we

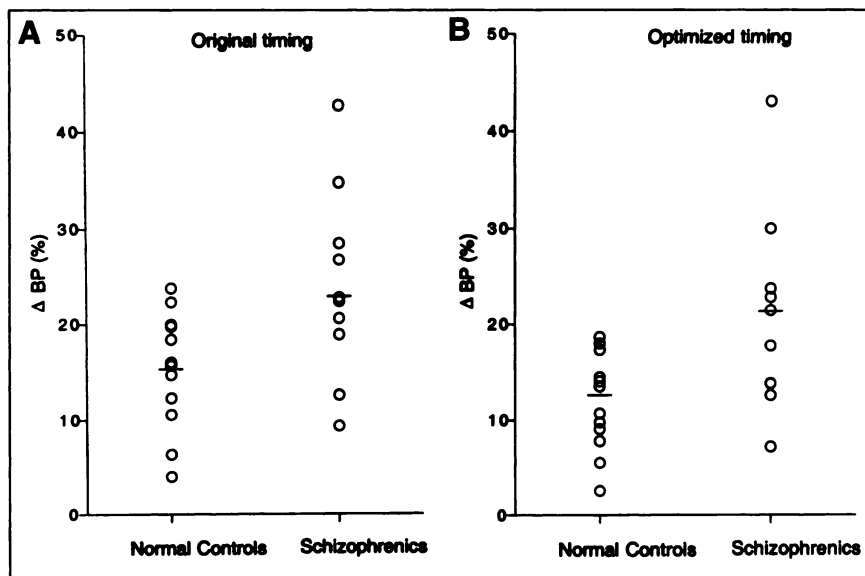


**FIGURE 3.** Optimal timing applied to human data from (6). Values shown are measurements of  $\Delta BP$  measured after 0.2 mg/kg dose of amphetamine in group of healthy volunteers ( $n = 12$ ) and group of patients with schizophrenia ( $n = 11$ ). (A) Original data. (B) Same data as in A processed with optimal timing.

used the parameters for the dopamine pulse that were derived from microdialysis studies of anesthetized rhesus monkeys (10). After the drop in the basal ganglia time-activity curve produced by amphetamine, the simulated concentration curve showed a return toward the baseline values (Fig. 2), an effect that was not detectable in the human data. This apparent discrepancy between simulated and modeled data may be associated with differences in the time course of the dopamine pulse between awake humans and anesthetized monkeys. For example, the duration of the dopamine pulse in humans may be longer than that in monkeys—i.e., a smaller dopamine clearance rate ( $r$ ). Alternatively, the extended receptor model may not adequately describe the features of the *in vivo* environment, including multiple affinity states and receptor internalization (18).

Some of the error in  $\Delta BP$  was associated with incomplete equilibrium. More rapid equilibrium could be achieved with the B/I method if the magnitude of the bolus component of the infusion ( $K_{bol}$  (9)) is adjusted. In the original human study (6),  $K_{bol}$  was 135 min—i.e., the bolus equaled 135 min worth of infusion—or 57% of the injection volume for a study of 100-min duration. We estimated an optimized  $K_{bol}$  with 2 approaches. One was by generating time-activity curves of the target and background regions with fixed kinetic parameters and the 11 plasma input curves that were modified with new  $K_{bol}$  values (analogous derivation in Appendix B). In the second approach, new time-activity curves were computed from measured time-activity curves of basal ganglia and cerebellum from 23 human studies. The optimal  $K_{bol}$  was chosen by least-squares fitting (9), and a value of 105 min was obtained in both cases. This suggests that the bolus component of the B/I method should be smaller and is consistent with the fact that the average basal ganglia time-activity curves slightly overshot the equilibrium values and then had a negative slope. For a 100-min study duration and a  $K_{bol}$  value of 105 min, the percentage of the dose volume injected as the bolus would be 51%.

Because of decay, the bolus will account for 79% of the radioactive dose.

This optimization approach is extendable to other receptor-activation studies using the B/I method. In addition, there may be other intervention studies in which this type of analysis and optimization may be applicable, even for radiopharmaceuticals that do not bind to receptors. For example, dynamic changes in tissue levels of amino acids that produce changes in the occupancy of the transporter could be traced with a radiolabeled nonmetabolized amino acid.

## CONCLUSION

This article defines methodology to optimize the timing of the measurement of dynamic changes in neurotransmitter,  $\Delta BP$ , from a [ $^{11}C$ ]raclopride study using the B/I method. By altering the timing of the pre- and postamphetamine scans to 39–50 and 58–100 min, respectively, the simulation predicted a 28% increase in the SNR. When applied to a study comparing healthy volunteers with patients with schizophrenia, the probability value for statistical significance improved from 0.038 to 0.012. This is equivalent to using the original timing and increasing the number of subjects from 12 to 17. Application of these approaches will be important in maximizing the usefulness of PET and SPECT ligands to detect subtle stimulus-induced changes in neurotransmitter levels.

## APPENDIX A

### Noise Model

Phantom and human data were used to develop a noise model for  $\Delta BP$  to optimize its measurement. First, noise in the background region was evaluated. Then, the noise in the target region was determined on the basis of background region noise and the target-to-background contrast. Finally, an error propagation analysis was used to determine the total error in  $\Delta BP$ .

A cylindrical phantom (16-cm diameter and 17-cm axial length) was used for the background radioactivity. Two 3-cm-diameter spheres (volume, 14 mL each), simulating the basal ganglia target region, were placed in the center of the phantom. The total activity in the phantom was kept at ~3 MBq based on the analysis of 16 human [<sup>11</sup>C]raclopride studies in which the total brain radioactivity at 40 min after injection was  $2.89 \pm 0.45$  MBq (injected radioactivity, ~300 MBq). Solutions of <sup>18</sup>F were used for the target and background regions of the phantom. The target-to-background radioactivity concentration ratio was varied from 1 to 11 starting with the highest contrast. Then, accounting for decay of <sup>18</sup>F, additional <sup>18</sup>F solution was added to the background so that the total radioactivity was kept at ~3 MBq.

We used an Advance PET scanner (General Electric Medical Systems, Waukesha, WI) operating in 3-dimensional mode, which has reconstructed transverse resolution of 6.4 mm and axial slice width of 6.0 mm (19). One image set contains 35 slices with voxel sizes of 2 mm in plane and 4.25 mm axially. At each contrast level, gated acquisition was performed to obtain 20 statistically equivalent image replicates, each with a duration of 1 min. Image reconstruction was performed using the clinical filter and corrections.

From the 20-replicate images, mean and SD images were generated. A background VOI was placed on slices 8–10, where the cerebellum is usually found in human studies. The VOI shape was a half cylinder with radius of 6 cm. The radius was chosen so that the VOI volume was similar to that used in the human analysis. Pixel SD for the background region ( $\sigma'_{PIX}$ ) was obtained from the mean value within the VOI on the SD image. VOI SD in the background region ( $\sigma'_{VOI}$ ) was calculated from 20 replicated VOI values. For the target regions, spherical VOIs were used to measure pixel noise ( $\sigma_{PIX}$ ) and VOI noise ( $\sigma_{VOI}$ ). To assess the effect of target VOI size, the radius of the spherical VOI was varied from 3 to 30 mm.

### Noise Model for Background Region

*Pixel Noise.* In Poisson statistics, the pixel coefficient of variation (CV) is equal to the inverse of the square root of counts. In reconstructed PET images, we computed pixel noise from 16 human PET [<sup>11</sup>C]raclopride studies by taking advantage of the multiple scan frames acquired during the pre- and poststimulus period. SD images for pre- and poststimulus were generated from the 30–50 min (5 frames) and 75–100 min (5 frames) time periods, and the following relationship between the CV of the background region (CV') and the NECR (13,14) was developed:

$$CV' = \frac{\sigma'_{PIX}}{C'} = \frac{691}{\sqrt{NECR \times \Delta t}}, \quad \text{Eq. 1A}$$

where  $C'$  is the radioactivity concentration in the background region averaged over the designated time period and  $\Delta t$  is the total duration of the scan frames. A lower scale factor (461) for Equation 1A was found when NEC data

from phantom studies were fit. This discrepancy may be associated with differences in emission and attenuation distributions between the phantom and human brain. Note, however, that the absolute value of this scale factor has no effect on the choice of optimized timing.

For purposes of simulation of noisy time–activity curves, we developed an empiric model for NECR as a function of time in [<sup>11</sup>C]raclopride studies. From averaged human NECR curves (normalized by injected radioactivity), NECR at time  $t$  (min) was described by the following equation:

$$\begin{aligned} \frac{NECR(t)}{\text{injected activity}} &= 2.78 \times 10^4 (e^{1.41t} - 1) \quad t < 1.77 \text{ min} \\ &= 3.27 \times 10^5 e^{-0.0297t} \quad t > 1.77 \text{ min}, \end{aligned} \quad \text{Eq. 2A}$$

with the exponential constant  $0.0297 \text{ min}^{-1}$  close to the decay constant of <sup>11</sup>C.

*VOI Noise.* Next, we considered the relationship between pixel noise ( $\sigma'_{PIX}$ ) and VOI noise ( $\sigma'_{VOI}$ ) in the background region. For a VOI with  $n'$  pixels, with  $c'_i$  being the individual pixel values, the variance of the VOI value is:

$$\sigma'^2_{VOI} = \frac{1}{n'^2} \sum_{i=1}^{n'} \sum_{j=1}^{n'} \text{Cov}(c'_i, c'_j). \quad \text{Eq. 3A}$$

Expressing covariance in terms of variance and correlations, and assuming that the correlation coefficients between 2 pixels depend only on their relative distance (20), Equation 3A becomes:

$$\sigma'^2_{VOI} \approx \frac{1}{n'^2} \sum_{i=1}^{n'} \sum_{j=1}^{n'} \rho(d_{ij}) \sqrt{\text{Var}(c'_i) \text{Var}(c'_j)}, \quad \text{Eq. 4A}$$

where  $\rho(d)$  is the mean correlation between pairs of pixels separated by distance  $d$ , and  $d_{ij}$  is the distance between pixels  $i$  and  $j$ . Approximating the individual pixel variances with the average pixel variance within the VOI ( $\sigma'^2_{PIX}$ ), Equation 4A becomes:

$$\sigma'^2_{VOI} \approx \frac{\sigma'^2_{PIX}}{n'^2} \sum_{i=1}^{n'} \sum_{j=1}^{n'} \rho(d_{ij}) \equiv \frac{\sigma'^2_{PIX}}{n'^2} P^2(n'), \quad \text{Eq. 5A}$$

where  $P(n)$  is the square root of the sum of correlation coefficients of each pair of pixels in the VOI. We calculated  $\rho(d)$  from sample correlation coefficients derived from the 20-replicate phantom images.  $P(n')$  values were tabulated for cylindrical VOIs with  $n'$  varying from 40 to 5800, and the resultant data were fitted to the following equation:

$$P(n') = 5.80 \times n'^{0.327}. \quad \text{Eq. 6A}$$

Combining Equations 1A, 5A, and 6A leads to the noise model for the background VOI:

$$\sigma'_{VOI} = \frac{4008 \times C'}{\sqrt{NECR \times \Delta t \times n'^{0.673}}}. \quad \text{Eq. 7A}$$

### Noise Model for Target Region

**Pixel Noise.** From previous studies of PET image noise (14,20–22), the local radioactivity concentration has only a small influence on pixel noise. Therefore, we investigated the relationship of pixel noise between the target ( $\sigma_{PIX}$ ) and background ( $\sigma'_{PIX}$ ) regions, and found the following relationship:

$$\sigma_{PIX} = 0.978 \times \sigma'_{PIX} R^{0.197}. \quad \text{Eq. 8A}$$

In application of this formula, we approximated R from measured VOI values of the target and background regions. The parameters were determined by fitting the average  $\sigma_{PIX}$  values obtained from a spherical VOI (radius = 1.5 cm) on the phantom SD image over the range of target-to-background contrasts. These results show a great deal of similarity to a myocardial noise analysis (Fig. 10 in Pajevic et al. (14)) with an exponent (Eq. 8A) of 0.152.

**VOI Noise.** The relationship between pixel and VOI noise ( $\sigma_{VOI}$ ) in the target region was derived from phantom noise values of spherical VOIs with different sizes (range of n, 11–7721), in a manner similar to that of the background region, and found to be

$$\sigma_{VOI} = 2.85 \frac{\sigma_{PIX}}{n^{0.5}}. \quad \text{Eq. 9A}$$

Combining Equations 8A, 9A, and 1A leads to the noise model for the target VOI:

$$\sigma_{VOI} = 1928 \frac{C'R^{0.197}}{\sqrt{NECR \times \Delta t \times n^{0.5}}}. \quad \text{Eq. 10A}$$

### Noise Model for $\Delta BP$

The SD of  $\Delta BP$  was derived by applying a propagation of error analysis to Equation 1:

$$\text{SD}(\Delta BP) = 100 \times \frac{R_{\text{post}} - 1}{R_{\text{pre}} - 1} \times \sqrt{\frac{\sigma_{\text{VOI,pre}}^2 / C_{\text{pre}}^2 + \sigma_{\text{VOI,pre}}'^2 / C_{\text{pre}}'^2}{(1 - R_{\text{pre}}^{-1})^2} + \frac{\sigma_{\text{VOI,post}}^2 / C_{\text{post}}^2 + \sigma_{\text{VOI,post}}'^2 / C_{\text{post}}'^2}{(1 - R_{\text{post}}^{-1})^2}}. \quad \text{Eq. 11A}$$

Substituting Equations 7A and 10A into Equation 11A yields the final model for the SD of  $\Delta BP$ , Equation 6.

## APPENDIX B

### Metabolite Correction For B/I Studies

In human studies, we found large uncertainties in the measurement of the plasma metabolite correction caused by limited counting statistics. Therefore, we used the average metabolite correction given by Lammertsma et al. (17). However, these data are based on bolus injection, and our studies used the B/I method. With constant infusion of tracer, the unmetabolized fraction at any time will be higher than that in a bolus study. This appendix presents the derivation of the B/I metabolite correction from the bolus values.

Let  $f(t)$  be the total plasma radioactivity and  $f^m(t)$  be the metabolite-corrected curve after a bolus injection. Fitting the unmetabolized fraction data of Figure 2 in (17) to a 2-exponential function of time (min) yields

$$\frac{f^m(t)}{f(t)} = 0.176e^{-0.250t} + 0.824e^{-0.0048t}. \quad \text{Eq. 1B}$$

For a B/I experiment of duration T, the infusion protocol can be expressed (9):

$$H(t) = \frac{K_{\text{bol}}\delta(t) + \theta(t) - \theta(t - T)}{K_{\text{bol}} + T}, \quad \text{Eq. 2B}$$

where  $K_{\text{bol}}$  is the bolus magnitude (135 min for these studies),  $\delta(t)$  is the Dirac  $\delta$  function, and  $\theta(t)$  is 0 for  $t < 0$  and 1 for  $t > 0$ . Let  $g(t)$  and  $g^m(t)$  be the total and metabolite-corrected plasma radioactivity for a B/I study, respectively. Assuming that peripheral metabolism is a linear, time-invariant process,  $g(t)$  can be obtained by convolution of  $f(t)$  and  $H(t)$ , i.e.,

$$g(t) = H(t) \otimes f(t) = \frac{K_{\text{bol}}f(t) + \int_0^t f(\tau) d\tau}{K_{\text{bol}} + T}. \quad \text{Eq. 3B}$$

Similarly,

$$g^m(t) = H(t) \otimes f^m(t) = \frac{K_{\text{bol}}f^m(t) + \int_0^t f^m(\tau) d\tau}{K_{\text{bol}} + T}. \quad \text{Eq. 4B}$$

From Equation 3B,  $f(t)$  can be determined from  $g(t)$  using Laplace transforms:

$$f(t) = \left(1 + \frac{T}{K_{\text{bol}}}\right) g(t) - \frac{1 + \frac{T}{K_{\text{bol}}}}{K_{\text{bol}}} g(t) \otimes e^{-(t/K_{\text{bol}})}. \quad \text{Eq. 5B}$$

Finally, the metabolite-corrected curve  $g^m(t)$  can be determined by substituting Equations 5B and 1B into Equation 4B:

$$g^m(t) = \frac{K_{\text{bol}} \left( \left(1 + \frac{T}{K_{\text{bol}}}\right) g(t) - \frac{1 + \frac{T}{K_{\text{bol}}}}{K_{\text{bol}}} g(t) \otimes e^{-(t/K_{\text{bol}})} \right) \times (0.176e^{-0.250t} + 0.824e^{-0.0048t})}{K_{\text{bol}} + T} + \frac{\int_0^t \left( \left(1 + \frac{T}{K_{\text{bol}}}\right) g(\tau) - \frac{1 + \frac{T}{K_{\text{bol}}}}{K_{\text{bol}}} g(\tau) \otimes e^{-(\tau/K_{\text{bol}})} \right) \times (0.176e^{-0.250\tau} + 0.824e^{-0.0048\tau}) d\tau}{K_{\text{bol}} + T}.$$

## ACKNOWLEDGMENTS

The authors thank Shielah Green for her technical assistance with the phantom experiment and acknowledge the helpful comments of Drs. Craig Barker and Peter Herscovitch.

## REFERENCES

1. Butcher SP, Fairbrother IS, Kelly JS, Arbuthnott GW. Amphetamine-induced dopamine release in the rat striatum: an in vivo microdialysis study. *J Neurochem*. 1988;50:346-355.
2. Innis RB, Malison RT, Al-Tikriti M, et al. Amphetamine-stimulated dopamine release competes in vivo for [<sup>125</sup>I]IBZM binding to the D2 receptor in nonhuman primates. *Synapse*. 1992;10:177-184.
3. Dewey SL, Smith GS, Logan J, Brodie JD, Fowler JS, Wolf AP. Striatal binding of the PET ligand <sup>11</sup>C-raclopride is altered by drugs that modify synaptic dopamine levels. *Synapse*. 1993;13:350-356.
4. Laruelle M, Abi-Dargham A, van Dyck CH, et al. SPECT imaging of striatal dopamine release after amphetamine challenge. *J Nucl Med*. 1995;36:1182-1190.
5. Laruelle M, Abi-Dargham A, van Dyck CH, et al. Single photon emission computerized tomography imaging of amphetamine-induced dopamine release in drug-free schizophrenic subjects. *Proc Natl Acad Sci USA*. 1996;93:9235-9240.
6. Breier A, Su T-P, Saunders R, et al. Schizophrenia is associated with elevated amphetamine-induced synaptic dopamine concentrations: evidence from a novel positron emission tomography method. *Proc Natl Acad Sci USA*. 1997;94:2569-2574.
7. Abi-Dargham A, Gil R, Krystal J, et al. Increased striatal dopamine transmission in schizophrenia: confirmation in a second cohort. *Am J Psychiatry*. 1998;155:761-767.
8. Koeppe MJ, Gunn RN, Lawrence AD, et al. Evidence for striatal dopamine release during a video game. *Nature*. 1998;393:266-268.
9. Carson RE, Channing MA, Blasberg RG, et al. Comparison of bolus and infusion methods for receptor quantitation: application to [<sup>18</sup>F]cyclofoxy and positron emission tomography. *J Cereb Blood Flow Metab*. 1993;13:24-42.
10. Endres CJ, Kolachana BS, Saunders RC, et al. Kinetic modeling of [<sup>11</sup>C]raclopride: combined PET-microdialysis studies. *J Cereb Blood Flow Metab*. 1997;17:932-942.
11. Carson RE, Breier A, Bartolomeis A, et al. Quantification of amphetamine-induced changes in [<sup>11</sup>C]raclopride binding with continuous infusion. *J Cereb Blood Flow Metab*. 1997;17:437-447.
12. Endres CJ, Carson RE. Assessment of dynamic neurotransmitter changes with bolus or infusion delivery of neuroreceptor ligands. *J Cereb Blood Flow Metab*. 1998;18:1196-1210.
13. Strother SC, Casey ME, Hoffman EJ. Measuring PET scanner sensitivity: relating countrates to image signal-to-noise ratios using noise equivalent counts. *IEEE Trans Nucl Sci*. 1990;37:783-788.
14. Pajevic S, Daube-Witherspoon ME, Bacharach SL, Carson RE. Noise characteristics of 3D and 2D PET images. *IEEE Trans Med Imag*. 1998;17:9-23.
15. Farde L, Eriksson L, Blomquist G, Halldin C. Kinetic analysis of central [<sup>11</sup>C]raclopride binding to D<sub>2</sub>-dopamine receptors studied by PET: a comparison to the equilibrium analysis. *J Cereb Blood Flow Metab*. 1989;9:696-708.
16. Press WH, Flannery BP, Teukolsky SA, Vetterling WT. *Numerical Recipes in C: The Art of Scientific Computing*. New York, NY: Cambridge University Press; 1988.
17. Lammertsma AA, Bench CJ, Hume SP, et al. Comparison of methods for analysis of clinical [<sup>11</sup>C]raclopride studies. *J Cereb Blood Flow Metab*. 1996;16:42-52.
18. Laruelle M, Iyer RN, Al-Tikriti MS, et al. Microdialysis and SPECT measurements of amphetamine-induced dopamine release in nonhuman-primates. *Synapse*. 1997;25:1-14.
19. Lewellen TK, Kohlmyer SG, Miyaoka RS, Kaplan MS. Investigation of the performance of the General Electric Advance positron emission tomograph in 3D mode. *IEEE Trans Nucl Sci*. 1996;43:2199-2206.
20. Carson RE, Yan Y, Daube-Witherspoon ME, Freedman N, Bacharach SL, Herscovitch P. An approximation formula for the variance of PET region-of-interest values. *IEEE Trans Med Imaging*. 1993;12:240-250.
21. Budinger TF, Derenzo SE, Greenberg WL, Gullberg GT, Huesman RH. Quantitative potentials of dynamic emission computed tomography. *J Nucl Med*. 1978;19:309-315.
22. Alpert NM, Chesler DA, Correia JA, et al. Estimation of the local statistical noise in emission computed tomography. *IEEE Trans Med Imaging*. 1982;1:142-146.